

Associated $J/\psi + \gamma$ diffractive production: the nature of Pomeron and test of hard diffractive factorization

Jia-Sheng Xu

Department of Physics, Peking University, Beijing 100871, China

Hong-An Peng

*China Center of Advance Science and Technology (World Laboratory), Beijing 100080, China
and Department of Physics, Peking University, Beijing 100871, China*

Abstract

We present a study of diffractive associated $J/\psi + \gamma$ production at the Fermilab Tevatron and LHC based on the Ingelman-Schlein model for hard diffractive scattering and the factorization formalism of NRQCD for quarkonia production. we find that this process ($p + \bar{p} \rightarrow p + J/\psi + \gamma + X$) can be used to probe the gluon content of the Pomeron and test the assumption of diffractive hard scattering factorization. Using the renormalized Pomeron flux factor $D \simeq 0.11(0.052)$, the single diffractive $J/\psi + \gamma$ production cross section at $4 < P_T < 10$ GeV, $-1 < \eta < 1$ region is found to be of the order of 3.0pb (8.5 pb). The ratio of single diffractive to inclusive production is 0.50%(0.15%) in central region at the Tevatron (LHC) for the gluon fraction in the Pomeron $f_g = 0.7$, independent of the values of color-octet matrix elements.

PACS number(s): 12.40Nn, 13.85.Ni, 14.40.Gx

1 Introduction

Early in the 1960's physicists already well realized that in high energy strong interaction the Regge trajectory with vacuum quantum number, the Pomeron, plays a particular and very important role in soft processes, such as the energy dependence of $\sigma_{tot}(s)$, the behavior of the elastic differential cross section $\frac{d\sigma^{el}}{dt}$ at small $|t|$, the single and double diffractive dissociation processes in hadron-hadron collisions [1]. After the advent of QCD, physicists begin to study the nature of the pomeron in the QCD framework [2]. Since the Pomeron carries the quantum number of the vacuum, in QCD language, it is a colorless entity, which leads to the diffractive events are characterized by a large rapidity gap, a region in rapidity devoiding of hadronic energy flow, this distinct class of events are observed by the ZEUS and H1 Collaboration at HERA in deep inelastic scattering region [3], which offer a unique chance to study the the soft scattering process with a hard virtual photon probe, therefore provide a more complete understanding of QCD .

In an original paper [4], It was suggested that hard diffractive scattering processes would give new and valuable insight about the nature of Pomeron. the Ingelman-Schlein (I-S) model assumes that the hard diffractive scattering processes can be calculated in a factorized way : first, a Pomeron is emitted from the diffractively scattered hadron, then partons of the Pomeron take part in hard subprocesses, the results will be diffractively produced high- P_T jets in $P - P(\bar{P}), \gamma - P$ collisions or larger rapidity gap events in diffractive deep inelastic scattering (DDIS), so the partonic struction of the Pomeron could be established and studied experimentally. These pridictions were confirmed subsequently. The UA8 Collaboration at CERN S $p\bar{p}$ S collider with $\sqrt{s} = 630$ GeV studied the diffractive jet distribution, indicates a dominant hard partonic structure of the Pomeron, however, the diffractive dijet event topology alone can not distinguish between a hard-quark or a hard-gluon struction in the Pomeron [5]. The DDIS and dijet photoproduction experiments at HERA have shed light on the partonic structure of the Pomeron. Combining the measurements of the diffractive structure function in DDIS and the photoproduction jet cross sections, the ZEUS Collaboration gives the first experimental evidence for the gluon content of the Pomeron and determines that the hard gluon fraction of the pomeron f_g is in the range $0.3 < f_g < 0.8$, independent of the validity of the momentum sum rule for the Pomeron and the normalization of the flux of Pomeron from the proton[6]. The H1 Collaboration also determines the fraction of the momentum of the Pomeron carried by the hard gluon, which is $f_g \sim 0.9$ at $Q^2 = 4.5$ GeV² and $f_g \sim 0.8$ at $Q^2 = 75$ GeV² [7]. The partonic structure of the Pomeron, based on the I-S model for hard diffraction, was also studied by the CDF Collaboration at the Tevatron through diffractive W production and dijet production [8] [9], which give further evidence for the hard partonic stucture of the Pomeron. Combining these two experiments, the CDF Collaboration determined the hard-gluon content of the Pomeron to be $f_g = 0.7 \pm 0.2$, this result is also independent of the Pomeron flux normalization or the validity of the momentum sum rule for the Pomeron.

However, there is a problem. The I-S model is based on the assumption of diffractive hard scattering factorization. Recently, a factorization theorem has been proven by Collins [10] for the lepton induced diffractive hard scattering processes, such as DDIS and diffractive

direct photoproduction of jets. This factorization theorem justifies the analysis given by the ZEUS and H1 Collaboration, and establishes the the universality of the diffractive parton distributions for those processes to which the theorem applies. In contrast, no factorization theorem has been established for diffractive hard scattering in hadron-hadron collisions. As already known before the advent of QCD, factorization fails for hard processes in diffractive hadron-hadron scattering [11]. Furthermore, in order to preserve the shapes of the M^2 and t distributions in soft single diffraction (SD) and predict correctly the experimentally observed SD cross section at all energy in $P\bar{P}$ collisions, Goulianos [12] has proposed to renormalize the Pomeron flux in an energy-dependent way, this approach indicates the breakdown of the triple-Regge theory for soft single diffractive exciation, and implies that diffractive hard factorization is likely breakdown in hadron-hadron collisions which appears to be confirmed by CDF experiments[8][9]. At large $|t|$, where perturbative QCD applies to the Pomeron, it was proven that there is a leading twist contribution which broken the factorization theorem for diffractive hard scattering in hadron-hadron collision [13]. Evidence for this substantial coherent perturbative contribution has been observed by the UA8 experiment in diffractive jet production, in which the square of the proton's four-momentum transfer t is in the region $-2 < t < -1 \text{ GeV}^2$ [5]. On the other hand, for the Pomeron at small $|t|$, nonperturbative QCD physics dominates, where the I-S model without much of a coherent contribution would be appropriate. Therefore, various hard diffractive processes may be considered to probe the partonic struction of the Pomeron, and test the hard diffractive factorization in hadron-hadron collisions [14] [15]. Recently, Alero *et al.*[16] extract the parton densities of the Pomeron from the HERA data on DDIS and diffractive photoproduction of jets, and use the fitted parton densities to predict the diffractive production of jets and weak bosons in $P\bar{P}$ collisions at the Tevatron. The predicted cross sections are substantially high than the experimental data, which signals a breakdown of hard scattering factorization in diffractive hadron-hadron collisions.

In this paper, we will discuss another diffractive process, the associated $J/\psi + \gamma$ single diffractive production at large P_T :

$$P + \bar{P} \rightarrow P + J/\psi + \gamma + X. \quad (1)$$

This process is of special significance because the produced large P_T J/ψ is easy to detect through its leptonic decay modes and the J/ψ 's large P_T is balance by the associated high energy photon. We will see through the following calculations, although the production cross section of associated $J/\psi + \gamma$ is sensitive to the color-octet matrix elements, the ratio of the single diffractive production cross section to the inclusive production cross section are not so. We find that the ratio is sensitive to the product Df_g , where D is the renormalization factor of the Pomeron flux(which indicates the factorization broken effects,)and f_g is the hard gluon fraction in the Pomeron. The measurement of this process at the Tevatron and LHC would shed light on the nature of the Pomeron and test the diffractive hard scattering factorization. Furthermore, this process is also interesting to the study of heavy quarkonium production mechanism.

Our paper is organized as follows. We describe in detail our calculation scheme in Sec.II. A brief introduction of the heavy quarkonium production mechanism, the hard subprocesses

for associated $J/\psi + \gamma$ production and a summary of the kinematics related to the J/ψ P_T distribution are given in this section. Our results and discussions are given in Sec. III.

2 Calculating Scheme

Based on the I-S model for diffractive hard scattering, the associated $J/\psi + \gamma$ single diffractive production process at large P_T consists of three steps (shown in Fig.1). First, the Pomeron is emitted from the proton with a small squared four-momentum transfer $|t|$. Second, partons from the anti-proton and the Pomeron scatter in the hard subprocesses that produce the almost point-like large P_T pair of $c\bar{c}$ and a associated photon. In the third step, J/ψ is produced from the point-like $c\bar{c}$ via soft gluon radiation.

2.1 Heavy quarkonium production mechanism

Prior to 1993, the conventional wisdom for heavy quarkonium production was based on the so-called color-singlet model (CSM)[17] which assumes that the heavy quark pair is produced in a color-singlet state with the right quantum numbers of the final heavy quarkonium in the hard subprocesses and the belief that the dominant production processes for color-singlet $c\bar{c}$ were the Feynman diagrams that were lowest order in α_s . However, at the Tevatron, the CSM prediction for prompt J/ψ production is an order of magnitude smaller than the CDF data at large P_T . The first major conceptual advance in heavy quarkonium production was the realization that fragmentation dominates at sufficiently large P_T [19] which indicates that most charmonium at large P_T is produced by the fragmentation of individual large P_T partons. The fragmentation functions are calculated in CSM, for example, the fragmentation function for $g \rightarrow J/\psi$ is calculated from the parton process $g \rightarrow c\bar{c} + gg$ in CSM. Including this fragmentation mechanism brings the theoretical predictions for prompt J/ψ production at Tevatron to within a factor of 3 of the data [20]. But the prediction for the ψ' remains a factor of 30 below the data even after including the fragmentation contribution (the ψ' “surplus” problem). Furthermore, the presence of the logarithmic infrared divergences in the production cross sections for P-wave charmonium states and the annihilation rate for $\chi_{cJ} \rightarrow q\bar{q}g$ indicate CSM is incomplete. All these problems indicate that some important production mechanism beyond CSM needs to be included [21][22]. And so the color-octet mechanism is proposed which is based on the factorization formalism of nonrelativistic quantum chromodynamics (NRQCD)[24][25]. Contrary to the basic assumption of CSM, the heavy quark pair in a color-octet state can bind to form heavy quarkonium.

Although the color-octet fragmentation picture of heavy quarkonium production [22] has provided valuable insight, the approximation that enter into fragmentation computations break down when a quarkonium’s energy becomes comparable to its mass. The fragmentation predictions for charmonium production are therefore unreliable at low P_T . In the case of Υ production, the exist data at the Tevatron are in the $P_T < 15$ GeV region, which significantly disagree with the fragmentation predictions. Based upon the above several recently developed ideas in heavy quarkonium physics, Cho and Leibovich[26] identify a

large class of color-octet diagrams that mediate quarkonia production at all energies, which reduce to the dominant set of gluon fragmentation graphs in the high P_T limit. By fitting the data of prompt J/ψ and Υ production at the Tevatron, numerical values for the long distance matrix elements are extracted, which are generally consistent with NRQCD power scaling rules [27]. In order to convincingly establish the color-octet mechanism, it is important to test whether the same matrix elements be able to explain heavy quarkonium production in other high energy processes, such as inclusive J/ψ production in e^+e^- annihilation on the Z^0 resonance and inelastic J/ψ photoproduction at HERA *et al.* .

2.2 The hard subprocesses for associated $J/\psi + \gamma$ production

J/ψ is described within the NRQCD framework in terms of Fock state decompositions as

$$\begin{aligned}
|J/\psi \rangle &= O(1) |c\bar{c}[{}^3S_1^{(1)}] \rangle + O(v) |c\bar{c}[{}^3P_J^{(8)}]g \rangle + \\
&O(v^2) |c\bar{c}[{}^1S_0^{(8)}]g \rangle + O(v^2) |c\bar{c}[{}^3S_1^{(1,8)}]gg \rangle + \\
&O(v^2) |c\bar{c}[{}^3P_J^{(1,8)}]gg \rangle + \dots,
\end{aligned} \tag{2}$$

where the $c\bar{c}$ pairs are indicated within the square brackets in spectroscopic notation. The pairs' color states are indicated by singlet (1) or octet (8) superscripts. The color octet $c\bar{c}$ state can make a transition into a physical J/ψ state by soft chromoelectric dipole (E1) transition(s) or chromomagnetic M1 transition(s)

$$(c\bar{c})[{}^{2S+1}L_j^{(1,8)}] \rightarrow J/\psi. \tag{3}$$

NRQCD factorization scheme [24] has been established to systematically separate high and low energy scale interactions. It is based upon a double power series expansion in the strong interaction fine structure constant $\alpha_s = \frac{g_s^2}{4\pi}$ and the small velocity parameter v . The production of a $(c\bar{c})[{}^{2S+1}L_j^{(1,8)}]$ pair with separation less than or of order $\frac{1}{m_c}$ are perturbatively computable. The long distance effects for the produced almost point-like $c\bar{c}$ to form the bound state are isolated into nonperturbative matrix elements. Furthermore, NRQCD power counting rules can be exploited to determine the dominant contributions to various quarkonium processes[27]. For direct J/ψ production, the color-octet matrix elements, $\langle 0 | \mathcal{O}_8^{J/\psi} [{}^3S_1] | 0 \rangle$, $\langle 0 | \mathcal{O}_8^{J/\psi} [{}^1S_0] | 0 \rangle$, $\langle 0 | \mathcal{O}_8^{J/\psi} [{}^3P_J] | 0 \rangle$ are all scaling as $m_c^3 v_c^7$. So these color-octet contributions to J/ψ production must be included for consistency.

The partonic level subprocesses for associated $J/\psi + \gamma$ production are composed of the gluon fusion subprocesses, which are sketched in Fig.2. These are

$$\begin{aligned}
g + g &\rightarrow \gamma + (c\bar{c})[{}^3S_1^{(1)}, {}^3S_1^{(8)}], \\
g + g &\rightarrow \gamma + (c\bar{c})[{}^1S_0^{(8)}, {}^3P_J^{(8)}].
\end{aligned} \tag{4}$$

The quark initiated subprocesses ($q\bar{q}$ channel) are strongly suppressed and will be neglected further. The color-singlet gluon-gluon fusion contribution to associated $J/\psi + \gamma$ production

is well known [28]:

$$\frac{d\hat{\sigma}}{d\hat{t}}(\text{singlet}) = \frac{\mathcal{N}_1}{16\pi\hat{s}^2} \left[\frac{\hat{s}^2(\hat{s} - 4m_c^2)^2 + \hat{t}^2(\hat{t} - 4m_c^2)^2 + \hat{u}^2(\hat{u} - 4m_c^2)^2}{(\hat{s} - 4m_c^2)^2(\hat{t} - 4m_c^2)^2(\hat{u} - 4m_c^2)^2} \right], \quad (5)$$

where

$$\hat{s} = (p_1 + p_2)^2, \quad \hat{t} = (p_2 - P)^2, \quad \hat{u} = (p_1 - P)^2. \quad (6)$$

The overall normalization \mathcal{N}_1 is defined as

$$\mathcal{N}_1 = \frac{4}{9}g_s^4 e^2 e_c^2 m_c^3 G_1(J/\psi), \quad (7)$$

where

$$G_1(J/\psi) = \frac{\langle 0 | \mathcal{O}_1^{J/\psi} [{}^3S_1] | 0 \rangle}{3m_c^2} = \frac{\Gamma(J/\psi \rightarrow j^+ l^-)}{\frac{2}{3}\pi e_c^2 \alpha^2} \quad (8)$$

and $e_c^2 = \frac{2}{3}$.

The average-squared amplitude of the subprocess $g + g \rightarrow \gamma + (c\bar{c})[{}^3S_1^{(8)}]$ can be obtained from the average-squared amplitude of $g + g \rightarrow \gamma + (c\bar{c})[{}^3S_1^{(1)}]$ by taking into account of different color factor. The result is

$$\begin{aligned} & \frac{d\hat{\sigma}}{d\hat{t}} [g + g \rightarrow \gamma + (c\bar{c})[{}^3S_1^{(8)}] \rightarrow \gamma + J/\psi] \\ &= \frac{1}{16\pi\hat{s}^2} \frac{15}{6} \bar{\Sigma} |M(g + g \rightarrow \gamma + (c\bar{c})[{}^3S_1^{(1)}])|^2 \cdot \frac{1}{24m_c} \langle 0 | \mathcal{O}_8^{J/\psi} [{}^3S_1] | 0 \rangle \\ &= \frac{1}{16\pi\hat{s}^2} \frac{15}{6} \frac{1}{8} \frac{1}{12} \cdot 64g_s^4 e_c^2 e^2 m_c^2 \left[\frac{\hat{s}^2(\hat{s} - 4m_c^2)^2 + \hat{t}^2(\hat{t} - 4m_c^2)^2 + \hat{u}^2(\hat{u} - 4m_c^2)^2}{(\hat{s} - 4m_c^2)^2(\hat{t} - 4m_c^2)^2(\hat{u} - 4m_c^2)^2} \right] \\ & \cdot \frac{1}{24m_c} \langle 0 | \mathcal{O}_8^{J/\psi} [{}^3S_1] | 0 \rangle. \end{aligned} \quad (9)$$

The average-squared amplitudes of the subprocesses $g + g \rightarrow \gamma + (c\bar{c})[{}^1S_0^{(8)}]$ and $g + g \rightarrow \gamma + (c\bar{c})[{}^3P_J^{(8)}]$ can be found in [29],

$$\begin{aligned} & \frac{d\hat{\sigma}}{d\hat{t}} [g + g \rightarrow \gamma + (c\bar{c})[{}^1S_0^{(8)}] \rightarrow \gamma + J/\psi] \\ &= \frac{1}{16\pi\hat{s}^2} \bar{\Sigma} |M(g + g \rightarrow \gamma + (c\bar{c})[{}^1S_0^{(8)}])|^2 \cdot \frac{1}{8m_c} \langle 0 | \mathcal{O}_8^{J/\psi} [{}^1S_0] | 0 \rangle, \\ & \frac{d\hat{\sigma}}{d\hat{t}} [g + g \rightarrow \gamma + (c\bar{c})[{}^3P_J^{(8)}] \rightarrow \gamma + J/\psi] \\ &= \frac{1}{16\pi\hat{s}^2} \sum_J \bar{\Sigma} |M(g + g \rightarrow \gamma + (c\bar{c})[{}^3P_J^{(8)}])|^2 \cdot \frac{1}{8m_c} \langle 0 | \mathcal{O}_8^{J/\psi} [{}^3P_0] | 0 \rangle, \end{aligned} \quad (10)$$

where the heavy quark spin symmetry

$$\langle 0 | \mathcal{O}_8^{J/\psi} [{}^3P_J] | 0 \rangle = (2J + 1) \langle 0 | \mathcal{O}_8^{J/\psi} [{}^3P_0] | 0 \rangle \quad (11)$$

is exploited.

2.3 The P_T distribution of J/ψ

Now we consider the P_T distribution of J/ψ produced in process

$$p(P_p) + \bar{p}(P_{\bar{p}}) \rightarrow p(P'_p) + J/\psi(P) + \gamma(k) + X. \quad (12)$$

Based on the I-S model for diffractive hard scattering, the differential cross section can be expressed as

$$d\sigma = f_{IP/p}(\xi, t) f_{g/IP}(x_1, Q^2) f_{g/\bar{p}}(x_2, Q^2) \frac{d\hat{\sigma}}{d\hat{t}} d\xi dt dx_1 dx_2 d\hat{t}, \quad (13)$$

where ξ is the momentum fraction of the proton carried by the Pomeron, $t = (P_p - P'_p)^2$ is the squared of the proton's four-momentum transfer. $f_{IP/p}(\xi, t)$ is the Pomeron flux factor

$$\begin{aligned} f_{IP/p}(\xi, t) &= \frac{d^2\sigma_{SD}/d\xi dt}{\sigma_T^{IPP}(s', t)} = \frac{\beta_1^2(0)}{16\pi} \xi^{1-2\alpha(t)} F^2(t) \\ &= K \xi^{1-2\alpha(t)} F^2(t), \end{aligned} \quad (14)$$

where the parameters are chosen as [12]

$$K = 0.73 GeV^2, \quad \alpha(t) = 1 + 0.115 + 0.26(GeV^{-2})t, \quad F^2(t) = e^{4.6t}. \quad (15)$$

In the following calculation, we use the renormalized flux factor for the Pomeron, proposed by Goulianos [12] in order to preserve the shapes of the M^2 and t distribution in soft single diffraction (SD) and predict correctly the observed SD cross section at all energies in $p\bar{p}$ collisions,

$$f_{IP/p}^{RN}(\xi, t) = D f_{IP/p}(\xi, t), \quad (16)$$

the renormalization factor D is defined as

$$D = Min(1, \frac{1}{N}) \quad (17)$$

with

$$N = \int_{\xi_{min}}^{\xi_{max}} d\xi \int_{-\infty}^0 dt f_{IP/p}(\xi, t), \quad (18)$$

where $\xi_{min} = \frac{M_0^2}{s}$ with $M_0^2 = 1.5 GeV^2$ (effective threshold) and $\xi_{max} = 0.1$ (coherence limit). At the Tevatron energy ($\sqrt{s} = 1800 GeV$), $D = \frac{1}{9}$.

We now consider the kinematics. In the $p\bar{p}$ c.m. frame, we can express the momenta of the incident p, \bar{p} and gluons *etc.* as

$$\begin{aligned} P_p &= \frac{\sqrt{s}}{2}(1, 1, \vec{0}) \\ P_{\bar{p}} &= \frac{\sqrt{s}}{2}(1, -1, \vec{0}) \end{aligned}$$

$$\begin{aligned}
P_{IP} &= \frac{\sqrt{s}}{2}\xi(1, 1, \vec{0}) \\
p_1 &= \frac{\sqrt{s}}{2}x_1\xi(1, 1, \vec{0}) = x_1P_{IP} \\
p_2 &= \frac{\sqrt{s}}{2}x_2(1, -1, \vec{0}) = x_2P_{\bar{p}}
\end{aligned} \tag{19}$$

where the first component is the energy, the second is longitudinal momentum, and the third is the transverse component of the four-momentum, x_1, x_2 are the momentum fractions of the gluons. The momenta of the outgoing J/ψ are given by

$$P = (E, P_L, P_T) = (E, P_T sh\eta, \vec{P}_T), \tag{20}$$

where P_T is the transverse momentum of J/ψ , η is the pseudo-rapidity of J/ψ and $E = \sqrt{m_\psi^2 + P_T^2 ch^2\eta}$.

The Mandelstam variables are defined as

$$\begin{aligned}
s &= (P_p + P_{\bar{p}})^2, \\
\hat{s} &= (p_1 + p_2)^2 = x_1 x_2 \xi s, \\
\hat{t} &= (p_2 - P)^2 = m_\psi^2 - \sqrt{s} x_2 (E + P_T sh\eta), \\
\hat{u} &= (p_1 - P)^2 = m_\psi^2 - \sqrt{s} x_1 \xi (E - P_T sh\eta).
\end{aligned} \tag{21}$$

Using $\hat{s} + \hat{t} + \hat{u} = m_\psi^2$, we have

$$x_2 = \frac{\sqrt{s}\xi x_1 (E - P_T sh\eta) - m_\psi^2}{x_1 \xi s - \sqrt{s}(E - P_T sh\eta)} \tag{22}$$

In order to obtain the distribution in the transverse momentum P_T for the process Eq.(12), we express the differential cross section as

$$d\sigma = f_{IP/p}^{RN}(\xi, t) f_{g/IP}(x_1, Q^2) f_{g/\bar{p}}(x_2, Q^2) \frac{d\hat{\sigma}}{d\hat{t}} J\left(\frac{x_1 x_2 \hat{t}}{x_1 \eta P_T}\right) d\xi dt dx_1 d\eta dP_T, \tag{23}$$

where the Jacobian can obtain from Eqs.(21) and Eq.(22),

$$J\left(\frac{x_1 x_2 \hat{t}}{x_1 \eta P_T}\right) = \frac{2s x_1 x_2 \xi P_T^2 ch\eta}{E[x_1 \xi s - \sqrt{s}(E + P_T sh\eta)]}. \tag{24}$$

Then the P_T distribution of J/ψ is expressed as

$$\frac{d\sigma}{dP_T} = \int_{\eta_{min}}^{\eta_{ma}} d\eta \int_{\xi_{dw}}^{\xi_{up}} d\xi \int_{x_{1min}}^{x_{1max}} dx_1 \int_{-1}^0 dt f_{IP/p}^{RN}(\xi, t) f_{g/IP}(x_1, Q^2) f_{g/\bar{p}}(x_2, Q^2) J\left(\frac{x_1 x_2 \hat{t}}{x_1 \eta P_T}\right) \frac{d\hat{\sigma}}{d\hat{t}}, \tag{25}$$

where the allowed regions of x_1, ξ are given by

$$\begin{aligned} x_{1min} &= \frac{E + P_T sh\eta - \frac{m_\psi^2}{\sqrt{s}}}{\xi(\sqrt{s} - E + P_T sh\eta)}, \\ \xi_{dw} &= \frac{E + P_T sh\eta - \frac{m_\psi^2}{\sqrt{s}}}{\sqrt{s} - E + P_T sh\eta}. \end{aligned} \quad (26)$$

In order to suppress the Reggon contributions, we set $\xi_{up} = 0.05$ as usual .

3 Numerical results and discussions

Now, we are ready to show the numerical results from the analytic expressions giving in the previous section. For numerical predictions we use $m_c = 1.5 GeV, \Lambda_4 = 235 MeV$, and set the factorization scale and the renormalization scale both equal to the transverse mass of J/ψ , *i.e.*, $Q^2 = m_T^2 = (m_\psi^2 + P_T^2)$. For the color-octet matrix elements $\langle 0 | \mathcal{O}_8^{J/\psi} [{}^3S_1] | 0 \rangle$, $\langle 0 | \mathcal{O}_8^{J/\psi} [{}^1S_0] | 0 \rangle$ and $\langle 0 | \mathcal{O}_8^{J/\psi} [{}^3P_0] | 0 \rangle$ we use the values determined by Beneke and Krämer [30] from fitting the direct J/ψ production data at the Tevatron [31] using GRV LO parton distribution functions,

$$\begin{aligned} \langle 0 | \mathcal{O}_8^{J/\psi} [{}^3S_1] | 0 \rangle &= 1.12 \times 10^{-2} GeV^3, \\ \langle 0 | \mathcal{O}_8^{J/\psi} [{}^1S_0] | 0 \rangle + \frac{3.5}{m_c^2} \langle 0 | \mathcal{O}_8^{J/\psi} [{}^3P_0] | 0 \rangle &= 3.90 \times 10^{-2} GeV^3. \end{aligned} \quad (27)$$

Since the matrix elements $\langle 0 | \mathcal{O}_8^{J/\psi} [{}^1S_0] | 0 \rangle$ and $\langle 0 | \mathcal{O}_8^{J/\psi} [{}^3P_0] | 0 \rangle$ are not determined separately, we present the two extreme values allowed by Eq.(27) as

$$\begin{aligned} {}^1S_0 \text{ saturated case :} & \quad \langle 0 | \mathcal{O}_8^{J/\psi} [{}^1S_0] | 0 \rangle = 3.90 \times 10^{-2} GeV^3 \\ & \quad \langle 0 | \mathcal{O}_8^{J/\psi} [{}^3P_0] | 0 \rangle = 0, \\ {}^3P_J \text{ saturated case :} & \quad \langle 0 | \mathcal{O}_8^{J/\psi} [{}^3P_0] | 0 \rangle = 1.11 \times 10^{-2} mc^2 GeV^3 \\ & \quad \langle 0 | \mathcal{O}_8^{J/\psi} [{}^1S_0] | 0 \rangle = 0. \end{aligned} \quad (28)$$

For the parton distribution functions, we use the GRV LO gluon distribution function for the anti-proton [32] and the hard gluon distribution function for the Pomeron [9]

$$x f_{g/IP}(x, Q^2) = f_g 6x(1-x), \quad f_g = 0.7 \pm 0.2. \quad (29)$$

We use the central value of f_g above for numerical calculation. We neglect any Q^2 evolution of the gluon density of the Pomeron at present stage.

With all ingredients set as above, in Fig.3 we show the P_T distribution $B \frac{d\sigma}{dP_T}$ for single diffractive $J/\psi + \gamma$ production in $p\bar{p}$ collisions at $\sqrt{s} = 1.8 TeV$, integrated over a pseudo-rapidity region $-1 \leq \eta \leq 1$ (central region). Where $B = 0.0594$ is the $J/\psi \rightarrow \mu^+ \mu^-$ leptonic decay branching ratio. The lower solid line is the color-singlet gluon-gluon fusion contribution, the lower dashed line represents ${}^1S_0^{(8)}$ -saturated color-octet contribution, the lower

dotted one is ${}^3P_J^{(8)}$ -saturated color-octet contribution and the lower dash-dot-dotted line is ${}^3S_1^{(8)}$ color-octet contribution. For comparison, we also calculate the inclusive associated $J/\psi + \gamma$ production $p + \bar{p} \rightarrow J/\psi + \gamma + X$ in the same kinematic region, the results are shown as the upper lines of Fig.3. The code for the lines are the same as the single diffractive production case. As shown in Fig.3, the color-octet ${}^3S_1^{(8)}$ contribution is strongly suppressed compared with the others over the entire P_T region considered in both production cases. The ${}^1S_0^{(8)}$ -saturated and ${}^3P_J^{(8)}$ -saturated contribution are smaller than the singlet contribution where $P_T < 5$ GeV, though their contribution dominate in the high P_T region, their differential cross section in the high P_T region is much smaller than that at low P_T region, so integrated over the P_T region, their contribution ($B\sigma = 0.08$ pb and 16 pb for ${}^1S_0^{(8)}$ -saturated contribution to SD and inclusive production respectively; $B\sigma = 0.06$ pb and 12 pb for ${}^3P_J^{(8)}$ -saturated contribution to SD and inclusive production respectively) are smaller than the color-singlet contribution ($B\sigma(singlet) = 0.10$ pb and 20 pb for SD and inclusive production respectively). The total SD (inclusive) production cross section at $\sqrt{s} = 1.8$ TeV, intergrated over $4 \leq P_T \leq 10$ Gev in central region is $B\sigma^{SD}(cen.) = 0.18$ pb ($B\sigma^{Inclusive}(cen.) = 36$ pb) for ${}^1S_0^{(8)}$ -saturated case, $B\sigma^{SD}(cen.) = 0.16$ pb ($B\sigma^{Inclusive}(cen.) = 32$ pb) for ${}^3P_J^{(8)}$ -saturated case. The ratio of the total SD production cross section to that of inclusive production in the central region $R^{cen.}$ are 0.50% for both ${}^1S_0^{(8)}$ -saturated case and ${}^3P_J^{(8)}$ -saturated case.

In Fig.4, we show the P_T distribution of J/ψ integrated over a pseudo-rapidity region $-4 \leq \eta \leq -2$ (forward region), at $\sqrt{s} = 1.8$ TeV, the code of lines is the same as Fig.3. One can find the differential cross section is significantly smaller than that in central region. So the diffractively produced J/ψ should be concentrated in the central detectors of collider. The same character was found early by Berger *et al.* [14] in the rapidity distribution of SD production of bottom and top quarks. This contrasts with the naive expectation that diffractively produced system appera only at large rapidity. The total SD (inclusive) production cross section at $\sqrt{s} = 1.8$ TeV, intergrated over $4 \leq P_T \leq 10$ GeV in forward region is $B\sigma^{SD}(fwd.) = 5.7 \times 10^{-2}$ pb ($B\sigma^{Inclusive}(fwd.) = 23$ pb) for ${}^1S_0^{(8)}$ -saturated case, $B\sigma^{SD}(fwd.) = 5.1 \times 10^{-2}$ pb ($B\sigma^{Inclusive}(fwd.) = 20$ pb) for ${}^3P_J^{(8)}$ -saturated case. The ratio of the total SD production cross section to that of inclusive production in the forward region $R^{fwd.}$ are 0.25% for both ${}^1S_0^{(8)}$ -saturated case and ${}^3P_J^{(8)}$ -saturated case.

In TABLE I., we show the ratio

$$R(P_T) = \frac{d\sigma^{SD}}{dP_T} / \frac{d\sigma^{Inclusive}}{dP_T} \quad (30)$$

at $\sqrt{s} = 1.8$ TeV in central region and forward region, where

$$\frac{d\sigma^{SD}}{dP_T} = \frac{d\sigma^{SD}(singlet)}{dP_T} + \frac{d\sigma^{SD}({}^3S_1^{(8)})}{dP_T} + \frac{d\sigma^{SD}({}^1S_0^{(8)})}{dP_T} \quad (31)$$

for ${}^1S_0^{(8)}$ -saturated case, and

$$\frac{d\sigma^{SD}}{dP_T} = \frac{d\sigma^{SD}(singlet)}{dP_T} + \frac{d\sigma^{SD}({}^3S_1^{(8)})}{dP_T} + \frac{d\sigma^{SD}({}^3P_J^{(8)})}{dP_T} \quad (32)$$

Table 1: The ratio $R(P_T)$ as a function of P_T at the Tevatron in central region ($-1 \leq \eta \leq 1$) $R^{cen.}(P_T)$ and forward region ($-4 \leq \eta \leq -2$) $R^{fwd.}(P_T)$.

P_T (GeV)	4	5	6	7	8	9	10
$R^{cen.}(P_T)(\%)$	0.52	0.52	0.50	0.48	0.47	0.46	0.44
$R^{fwd.}(P_T)(\%)$	0.28	0.28	0.28	0.28	0.29	0.29	0.30

for ${}^3P_J^{(8)}$ -saturated case.

The ratio $R(P_T)$ for ${}^1S_0^{(8)}$ -saturated case is the same as that for ${}^3P_J^{(8)}$ -saturated case. From this table, we can see that $R(P_T)$ is almost constant for $P_T \leq 6$ GeV both in central and forward regions. $R(P_T)$ varies slowly as P_T increase. Because the differential cross section in the high P_T region is much small than that at low P_T region, integrated over the overall P_T region, the ratios $R^{cen.}$ and $R^{fwd.}$ are not sensitive to the P_T smearing effects. Furthermore, we have varied the color-octet matrix elements $\langle 0 | \mathcal{O}_8^{J/\psi} [{}^3S_1] | 0 \rangle$, $\langle 0 | \mathcal{O}_8^{J/\psi} [{}^1S_0] | 0 \rangle + \frac{3.5}{m_c^2} \langle 0 | \mathcal{O}_8^{J/\psi} [{}^3P_0] | 0 \rangle$ by multiplied them by a factor between $\frac{1}{10}$ and 2, the result ratios $R^{cen.}$ and $R^{fwd.}$ is the same. This character demonstrates that the ratios $R^{cen.}$ and $R^{fwd.}$ are not sensitive to the values of color-octet matrix elements. The ratios $R^{cen.}$ and $R^{fwd.}$ are proportional to Df_g , hence are sensitive to the gluon fraction of the Pomeron f_g and the renormalization factor D which indicates the factorization broken effects. From other single diffractive production experiments, f_g can be determined, as the CDF Collaboration at Tevatron and the ZEUS Collaboration at HERA DESY have done, the renormalization factor D can be determined precisely from those ratios, *vice versa*. So measuring these ratios can probe the gluon density in the Pomeron and shed light on the test of diffractive hard scattering factorization theorem.

In Fig.5, we show the P_T distribution of J/ψ integrated over a pseudo-rapidity region $-1 \leq \eta \leq 1$ (central) at LHC energy $\sqrt{s} = 14$ TeV with the factor $D = 0.052$ calculated from Eq.(17). The code of lines is the same as Fig.3. As expected, the increasing of the differential cross section with c.m energy is slowed down by the renormalization of the Pomeron flux. The total SD (inclusive) production cross section at $\sqrt{s} = 14$ TeV, intergrated over $4 \leq P_T \leq 10$ GeV in central region is $B\sigma^{SD}(cen.) = 0.51$ pb ($B\sigma^{Inclusive}(cen.) = 3.4 \times 10^2$ pb) for ${}^1S_0^{(8)}$ -saturated case, $B\sigma^{SD}(cen.) = 0.46$ pb ($B\sigma^{Inclusive}(cen.) = 3.0 \times 10^2$ pb) for ${}^3P_J^{(8)}$ -saturated case. The ratio of the total SD production cross section to that of inclusive production in the central region $R^{cen.}$ are 0.15% for both ${}^1S_0^{(8)}$ -saturated case and ${}^3P_J^{(8)}$ -saturated case.

In the above calculations, we have set the values of factor D according to Eq.(17), it is $\frac{1}{9}$ at Tevatron energy and 0.052 at LHC energy. But the value is not unique, since it may change with different choice of the parameters such as M_0 and ξ_{max} in Eq.(18). If we use the central value of $D = 0.18 \pm 0.04$ measured by the CDF Collaboration at the Tevatron, the predicted ratio in the forward region $R^{fwd.}$ at the Tevatron, taking into account both p, \bar{p} can be diffractively scattered, will be 0.81%, which is close to the measured rate of diffractive dijet production with two jets of $E_T > 20$ GeV, $1.8 < |\eta| < 3.5$ and $\eta_1 \eta_2 > 0$.

Experimentally, the nondiffractive background to the diffractive associated $J/\psi + \gamma$ production must be dropped out in order to obtain useful information about the nature of Pomeron and the factorization broken effects, this can be attained by performing the rapid gap analysis in the CDF diffractive dijet experiment.

In conclusion, in this paper we have shown that the diffractive associated $J/\psi + \gamma$ production at large P_T is sensitive to the gluon content of the Pomeron and the factorization broken effects in hard diffractive scattering. Though the single diffractive and inclusive production cross section is sensitive to the values of color-octet matrix elements, the ratio of single diffractive to inclusive $J/\psi + \gamma$ production is not so and proportional to Df_g , hence are sensitive to the gluon fraction of the Pomeron f_g and the renormalization factor D which indicates the factorization broken effects. So experimental measurement of this ratio at the Tevatron and LHC can shed light on the nature of Pomeron and test the assumption of diffractive hard scattering factorization.

Acknowledgments

We thank Professor Kuang-Ta Chao and Dr. Feng Yuan for their reading of the manuscript and useful discussions. This work is supported in part by the National Natural Science Foundation of China, Doctoral Program Foundation of Institution of Higher Education of China and Hebei Natural Province Science Foundation, China.

References

- [1] P.D.B. Collins, *An introduction to Regge theory and High Energy Physics* (Cambridge University Press, Cambridge, England, 1977).
K. Goulianos, Phys. Rep. **101**, 169 (1985).
- [2] S.Nussinov, Phys. Rev. Lett. **34**, 1286 (1975) ; Phys. Rev. **D 14**, 246 (1976)
F. E. Low , Phys. Rev. **D 12**, 163 (1975)
- [3] M. Derrick *et al.*, ZEUS Collaboration, Phys. Lett. **B 315**, 481 (1993); *ibid.* **B332**,228 (1994); T.Ahmed *et al.*, H1 Collaboration, Nucl. Phys. **B 429**, 477 (1994)
- [4] G. Ingelman and P.E. Schlein , Phys. Lett. **B 152**, 256 (1985)
- [5] A. Brandt *et al.*, UA8 Collaboration, Phys. Lett. **B 297**, 417 (1992) ; R. Bonino *et al.*, *ibid.* **B 211**, 239 (1988)
- [6] M. Derrick *et al.*, ZEUS Collaboration, Z. Phys. **C 68**, 569 (1995) ; M. Derrick *et al.*, ZEUS Collaboration, Phys. Lett. **B 356**, 129 (1995)
- [7] T. Ahmed *et al.*, H1 Collaboration, Phys. Lett. **B 348**, 681 (1995) ; Z. Phys. **C 76**, 613 (1997) (hep-ex/9708016)

- [8] F. Abe *et al.*, CDF Collaboration, Phys. Rev. Lett. **78**, 2698 (1997)
- [9] F. Abe *et al.*, CDF Collaboration, Phys. Rev. Lett. **79**, 2636 (1997)
- [10] J.C. Collins, Phys. Rev. **D 57**, 3051 (1998)
- [11] P.V. Landshoff and J.C. Polkinghorne , Nucl. Phys. **B 33**, 221 (1971) ; F. Henyey and R. Savit, Phys. Lett. **B 52**, 71 (1974) ; J.L. Cardy and G.A. Winbow, Phys. Lett. **B 52**, 95 (1974) ; C.E. De Tar , S.D. Ellis and P.V. Landshoff, Nucl. Phys. **B 87**, 176 (1975)
- [12] K. Goulianos , Phys. Lett. **B 358**, 379 (1995); Erratum: *ibid.* **B 363**, 268 (1995) ; K. Goulianos and J. Montanha, hep-ph/9805496
- [13] J.C. Collins, L. Frankfurt and M. Strikmam, Phys. Lett. **B 307**, 161 (1993)
- [14] E.L. Berger, J.C. Collins, D.E. Soper and G. Stermam, Nucl. Phys. **B 286**,704 (1987)
- [15] P. Bruni and G. Ingelman, Phys. Lett. **B 311**, 317 (1993) ;
J.C. Collins *et al.*, Phys. Rev. **D 51**, 318 (1995) ;
Hong-An Peng, Ke-Cheng Qin and Zhen-Min He , High Energy Phys. and Nucl. Phys.(in Chinese) , **18**, No.12, 1078 , *ibid.* (in English), **19**, No.1, 31 (1995) ;
Hong-An Peng, Ke-Cheng Qin and Zhen-Min He , High Energy Phys. and Nucl. Phys.(in Chinese), **19**, No.1, 34 (1995), *ibid.* (in English), **19**, No.1, 51 (1995) ;
Feng Yuan and Kuang-Ta Chao, Phys. Rev. **D 57**, 5658 (1998)
- [16] L. Alvero, J.C. Collins, J. Terron, and J.J. Whitmore, hep-ph/9805268; L. Alvero, J.C. Collins and J.J. Whitmore, hep-ph/9806340
- [17] Chao-Hsi Chang, Nucl. Phys. **B 172**, 425 (1980) ; E. L. Berger and D. Jones: Phys. Rev. **D 23**, 1512 (1981) ; R. Baier and R. Rukel: Z. Phys. **C19** 251 (1983)
- [18] C. Albajar *et al.*, UA1 Collaboration, Phys. Lett. **B 256**, 112 (1991)
- [19] E. Braaten and T.C. Yuan, Phys. Rev. Lett. **71**, 1673 (1993)
- [20] E. Braaten, M.A. Doncheski, S. Fleming and M. Mangano, Phys. Lett. **B 333**, 548 (1994) ; M. Cacciari and M. Greco, Phys. Rev. Lett. **73**, 1586 (1994) ; D.P. Roy and K. Sridhar, Phys. Lett. **B 339**, 141 (1994)
- [21] G.T. Bodwin, E. Braaten and G.P. Lepage, Phys. Rev. **D 46**, R1914 (1992); *ibid.* **D 46**, R3703 (1992);
- [22] E. Braaten and S. Fleming, Phys. Rev. Lett. **74**, 3327 (1995);
- [23] For a recent review, see E. Braaten, S. Fleming and T.C. Yuan, Annu. Rev. Nucl. Part. Sci. **46**, 197 (1996); hep-ph/9602374

- [24] G.T. Bodwin, E. Braaten and G.P. Lepage, Phys. Rev. **D 51**, 1125 (1995); Erratum: *ibid.* **D 55**, 5853 (1997)
- [25] W.E. Caswell and G.P. Lepage, Phys. Lett. **B167**, 437 (1986)
- [26] P. Cho and A.K. Leibovich, Phys. Rev. **D 53**,150 (1996) ; *ibid.* **D 53**, 6203 (1996)
- [27] G.P. Lepage, L. Magnea, C. Nakhleh, U. Magnea and K. Hornbostel, Phys. Rev. **D 46**, 4052 (1992)
- [28] E. L. Berger and D. Jones: Phys. Rev. **D 23**, 1512 (1981) ;
- [29] C.S. Kim, Jungil Lee and H.S. Song, Phys. Rev. **D 55**, 5429 (1997); P. Ko, Jungil Lee and H.S. Song, Phys. Rev. **D 54**, 4312 (1996)
- [30] M. Beneke and M. Krämer, Phys. Rev. **D 55**, R5269 (1997)
- [31] F. Abe *et al.*, CDF Collaboration, Phys. Rev. Lett. **79**,578 (1997)
- [32] M. Glück, E. Reya and A. Vogt, Z. Phys. **C 67**, 433 (1995)

Figure Captions

Fig.1. Sketch diagram for diffractive associated $J/\psi + \gamma$ production in the Ingelman-Schlein model for diffractive hard scattering.

Fig.2. The subprocess $g_1 + g_2 \rightarrow \gamma + c\bar{c}[{}^{2S+1}L_J^{(1,8)}] \rightarrow \gamma + J/\psi$ in the NRQCD framework.

Fig.3. Transverse momentum of $J/\psi(P_T)$ distribution $Bd\sigma/dP_T$, integrated over the J/ψ pseudo-rapidity range $|\eta| \leq 1$ (central region), for single diffractive (lower) and inclusive (upper) associated $J/\psi + \gamma$ production at the Tevatron. Here B is the branching ratio of $J/\psi \rightarrow \mu^+\mu^-$ ($B = 0.0594$). The solid line is the color-singlet gluon-gluon fusion contribution, the dashed line represents ${}^1S_0^{(8)}$ -saturated color-octet contribution, the dotted one is ${}^3P_J^{(8)}$ -saturated color-octet contribution and the dot-dot-dashed line is ${}^3S_1^{(8)}$ color-octet contribution.

Fig.4. Transverse momentum of $J/\psi(P_T)$ distribution $Bd\sigma/dP_T$, integrated over the J/ψ pseudo-rapidity range $-4 \leq \eta \leq -2$ (forward region), for single diffractive (lower) and inclusive (upper) associated $J/\psi + \gamma$ production at the Tevatron. Here B is the branching ratio of $J/\psi \rightarrow \mu^+\mu^-$ ($B = 0.0594$). The solid line is the color-singlet gluon-gluon fusion contribution, the dashed line represents ${}^1S_0^{(8)}$ -saturated color-octet contribution, the dotted one is ${}^3P_J^{(8)}$ -saturated color-octet contribution and the dot-dot-dashed line is ${}^3S_1^{(8)}$ color-octet contribution.

Fig.5. Transverse momentum of $J/\psi(P_T)$ distribution $Bd\sigma/dP_T$, integrated over the J/ψ pseudo-rapidity range $|\eta| \leq 1$ (central region), for single diffractive (lower) and inclusive (upper) associated $J/\psi + \gamma$ production at LHC. Here B is the branching ratio of $J/\psi \rightarrow \mu^+\mu^-$ ($B = 0.0594$). The solid line is the color-singlet gluon-gluon fusion contribution, the dashed line represents ${}^1S_0^{(8)}$ -saturated color-octet contribution, the dotted one is ${}^3P_J^{(8)}$ -saturated color-octet contribution and the dot-dot-dashed line is ${}^3S_1^{(8)}$ color-octet contribution.

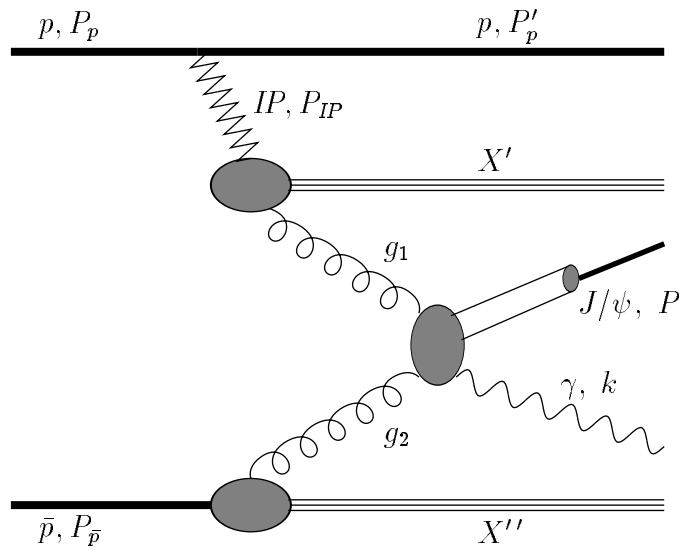


Fig.1

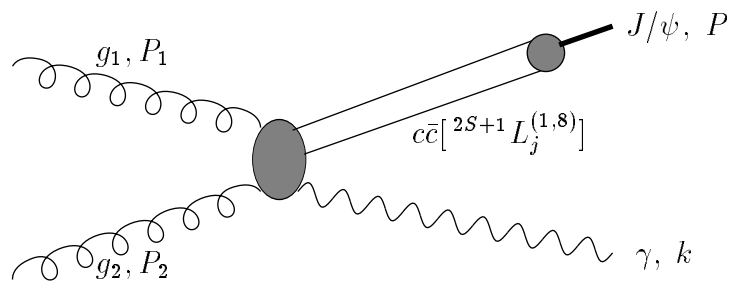


Fig.2

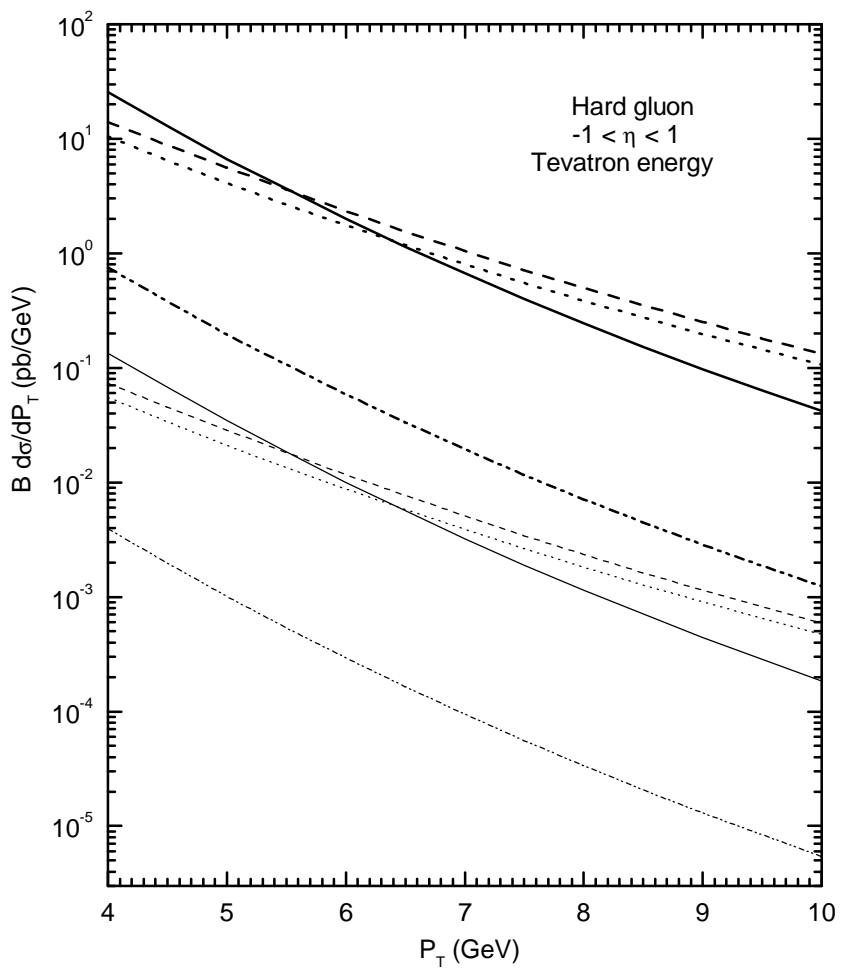


Fig.3

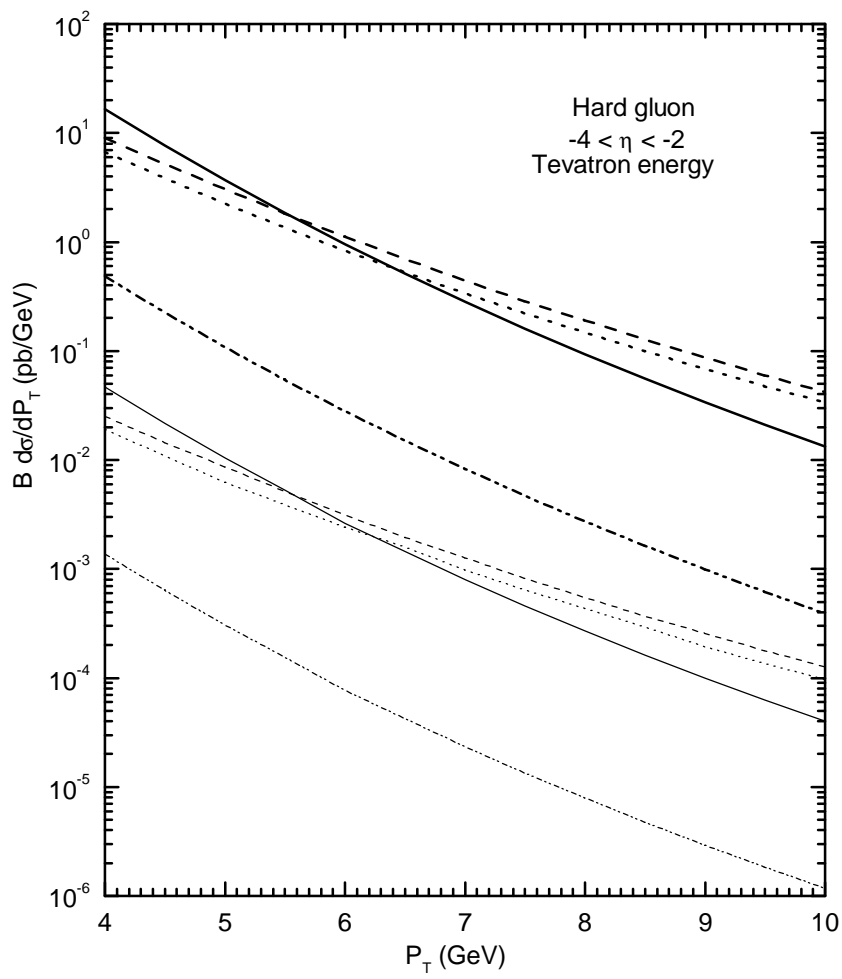


Fig. 4

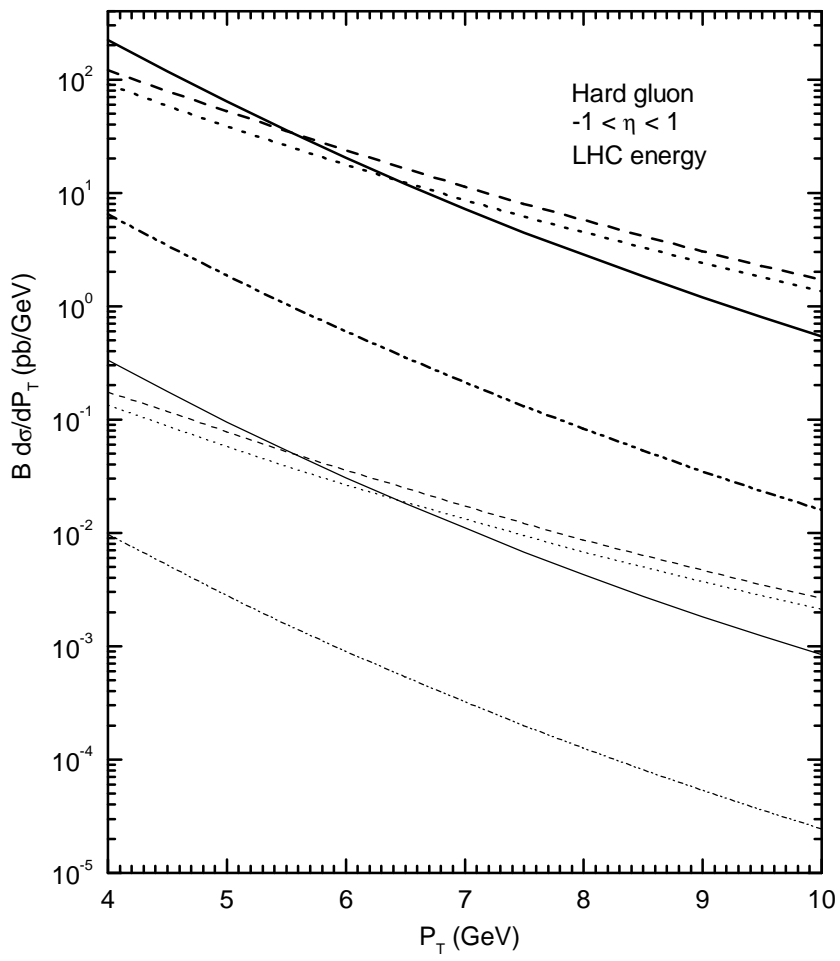


Fig.5